B. THE DYNAMICS OF GLIDE

We shall now turn from the crystallographic to the mechanical aspect of the phenomenon of glide. We shall describe the laws governing the initiation and continuation of glide, with special

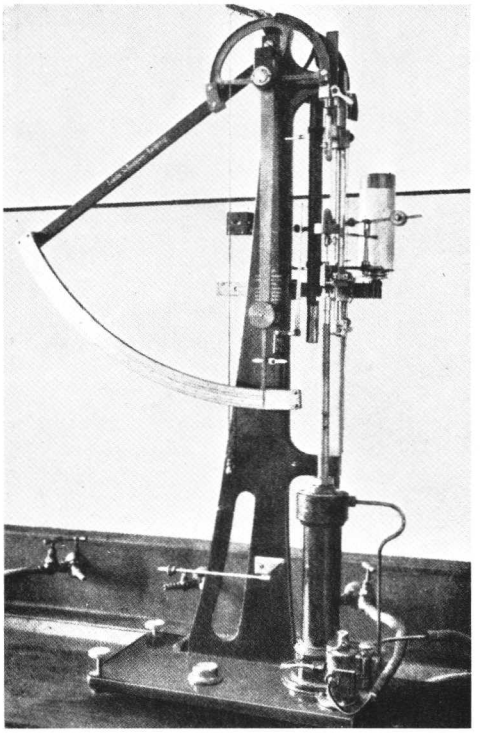

FIG. 74.—Schopper Tensile-testing Machine with Device for Automatically Recording the Stress–Strain Curve.

reference to the effect of alloying (the degree of purity), and to the time factor.

We shall confine our attention mainly to the common tensile test—a particularly simple type of loading—and shall deal only briefly with the behaviour of crystals subjected to more complicated types of stress.

Two types of apparatus which are much used for testing the tensile properties of wire-shaped metal crystals are illustrated in Figs. 74

and 75. The Schopper instrument records the stress–strain diagram automatically. With the filament-extension apparatus the load is determined from the deflection of a piece of steel sheet carrying the upper grip (mirror-reading), while the amount of extension is

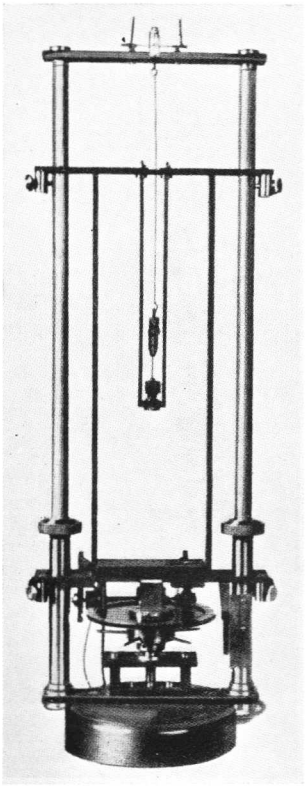

FIG. 75.—Filament-extension Apparatus—Polanyi (164).

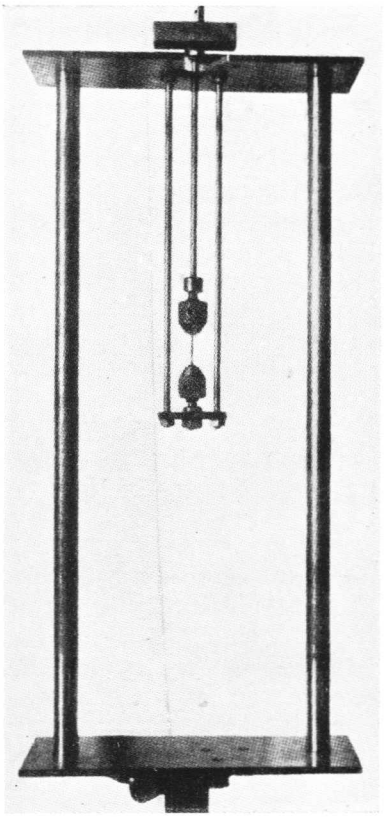

FIG. 76.—Adaptor for Carrying Out Extension Tests in the Schopper Tensometer in Baths of the Required Temperature (165).

measured by means of a micrometer screw attached to the lower grip. As shown in Fig. 75, the apparatus is also suitable for carrying out tests at temperatures other than room temperature. In the Schopper tensile machine by means of the adaptor illustrated in Fig. 76 the specimen can also be wholly immersed in a bath of the temperature required.

(*a*) FUNDAMENTAL LAWS

Fig. 77 represents a stress–strain curve with the usual co-ordinates —stress per square millimetre referred to the initial cross-section, and extension—such as is obtained when metal crystals are extended by glide. The process of deformation exhibits two clearly marked phases. In the first the stress increases sharply, while extension remains mainly within the elastic limit. Then the second phase begins, usually abruptly, and is characterized by *substantial* plastic deformation at only slightly increasing stress, until finally the crystal breaks.

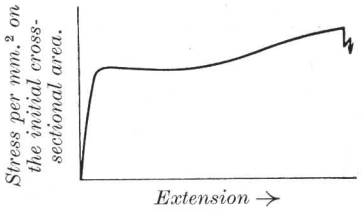

FIG. 77.—Normal Shape of the Stress–Strain Curve of Metal Crystals.

40. *Initiation of Glide in the Tensile Test (Yield Point). The Critical Shear Stress Law*

The initial parts of two stress–strain curves for cadmium crystals are shown in Fig. 78, in which the extension has been plotted on a very large scale. It is seen that a phase of very pronounced work hardening (steep increase in stress accompanied by slight increase in extension) is suddenly followed by a phase of appreciable extension with only a slight increase in stress. The transition is so abrupt that a physical significance may be justifiably attached to the stress at which this sudden glide occurs (166); it is termed "yield point of the crystal". It is seen that the yield point of a metal crystal, unlike that of the polycrystalline material, is not fixed by convention (0·2 per cent. plastic extension), but is determined by the nature of the deformation process itself. Nothing certain is yet known about

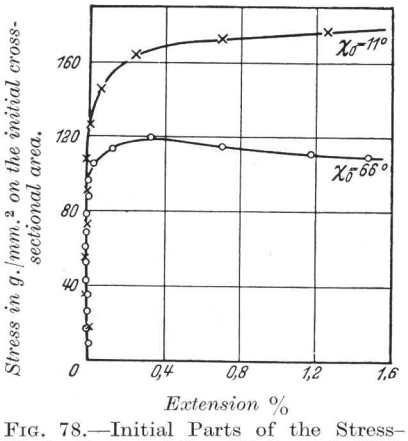

FIG. 78.—Initial Parts of the Stress–Strain Curves of Two Cd Crystals (170).

the plastic deformation which precedes the yield point. This is primarily due to the fact that strain does not take place uniformly over the whole length of the crystal under examination, but starts instead with local contractions, as shown in Fig. 79.

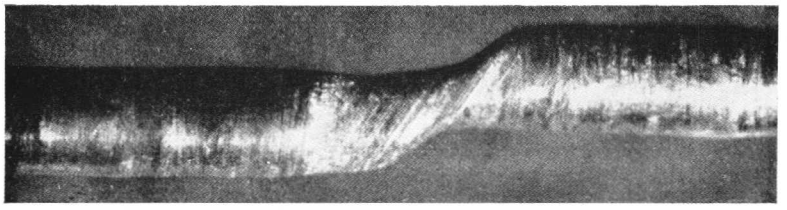

FIG. 79.—Start of Extension, by Necking, of a Cd Crystal.

The yield point of metal crystals is clearly marked in other ways too. Fig. 80 shows this by means of flow curves obtained with a cadmium crystal which was exposed to various initial stresses in the filament extension apparatus. It indicates that the speed of flow increases suddenly at a given stress, and that any substantial increase above this stress is quite impossible. Table VIII reveals that the yield point obtained in this way agrees closely with that which results from the stress–strain curve.

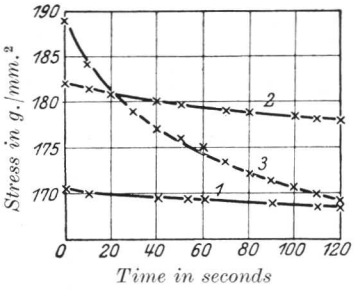

FIG. 80.—Flow Curves of a Cadmium Crystal. The Reduction in Stress is a Measure of the Increase in Length (170).

It has been found that this yield point is by no means constant for crystals of a given material, but strongly depends on the orientation of the crystal lattice to the direction of the applied stress. In the case of hexagonal magnesium the yield point of a crystal oriented to give maximum strength is forty times that of the weakest crystal. The differences with cubic metal crystals are much less pronounced, though still discernible.

If, in keeping with the process of deformation, the stress operative in yield-point tests (σ_0) is resolved into two components, a shear stress (S_0) in the direction of glide (t), on the glide plane (T), and a

normal stress (N_0) on T, the following two expressions are obtained (cf. Fig. 39) :

$$S_0 = \sigma_0 \sin \chi_0 \cos \lambda_0 \quad . \quad . \quad . \quad . \quad . \quad (40/1)$$
$$N_0 = \sigma_0 \sin^2 \chi_0 \quad . \quad . \quad . \quad . \quad . \quad . \quad (40/2)$$

in which χ_0 or λ_0 represent the angles between the direction of the pull and the glide plane or direction respectively.

Experimental studies of the relationship between yield point and

TABLE VIII

Comparison of the Yield Points of Cadmium Crystals obtained from Flow Curves and Stress–Strain Curves

Angle between the glide plane and the direction of pull.	Yield point (g./mm.²) obtained from	
	flow curve.	stress–strain curve.*
21·3°	155	159
23·5°	189	178
28·8°	158	136
43·3°	106 114	115
44·8°	87 83	99

* The figures given represent the mean of 2 to 4 determinations on portions of the same crystal.

the orientation of the glide elements have led to the conclusion that a *critical value of the resolved shear stress is required for the initiation of glide on a substantial scale* (Critical Shear Stress Law (166)). It has been found that the normal stress operating on the glide plane—a stress for which differences up to 1 : 2500 have been recorded—is of no importance ; this fact had also been ascertained by direct methods using tensile tests under hydrostatic pressure (up to 40 metric atmospheres) (167).

Fig. 81 gives the results of tests carried out to determine the influence of orientation on the yield point of hexagonal metal crystals. The differences in this case are very considerable, owing to the uniqueness of the basal glide plane. In these diagrams the yield point is plotted above the product $\sin \chi_0 \cos \lambda_0$, which gives the orientation of the glide elements. The left half of the diagrams refers to angles between the glide plane and the direction of tension,

of 0–45°; the right half to χ_0 values between 45° and 90°. The minimum values for the yield point are obtained when the glide elements are in positions of 45° to the direction of tension. The variation of the yield point, calculated on the assumption of a constant critical shear stress, is shown as an unbroken curve obtained from formula (40/1). This theoretical curve is an equilateral hyperbola which, in accordance with our diagram, is reflected on the ordinate which passes through the abscissa at 0·5. In all cases, the agreement with observed results is satisfactory.

With cubic crystals the orientation possibilities of the operative glide system are much more restricted. In this case there are no " unique " planes; consequently, if the geometrical position of a glide system is unfavourable a crystallographically equivalent system in a more favourable position always becomes available. The choice of the operative glide system for octahedral glide (T = (111), $t = [10\bar{1}]$) for different orientations of the direction of stress has already been shown in Fig. 61. The experimental results obtained with cubic face-centred metals [a copper–aluminium alloy (172), α-brass (containing 72 per cent. copper) (173), silver, gold, and their alloys (174), and nickel and nickel–copper alloys (175)] agree very well with the Critical Shear Stress Law. Deviations occur only when the orientation is such that the simultaneous operation of several glide systems disturbs the progress of simple glide. With crystals of pure aluminium, permanent set was usually observed to begin very gradually; recently, however, a clearly defined yield point has been found in this case too, although it is confined to crystals produced by recrystallization. With crystals of cast aluminium a permanent set was observed as soon as any stress was applied (171).

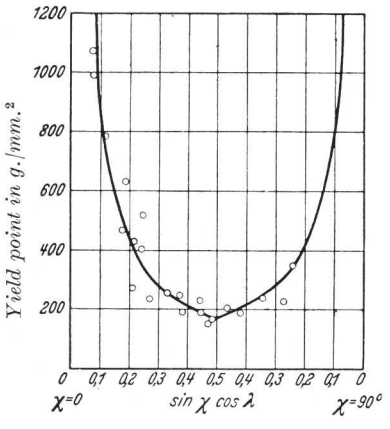

FIG. 81 (*a*) Magnesium (168).

Fig. 82 shows the experimentally determined dependence of the yield point on the orientation for *cubic body-centred α-iron* crystals. The observed differences are compatible with the validity of the

Critical Shear Stress Law for the most probable glide system ($T = (123)$, $t = [11\bar{1}]$).

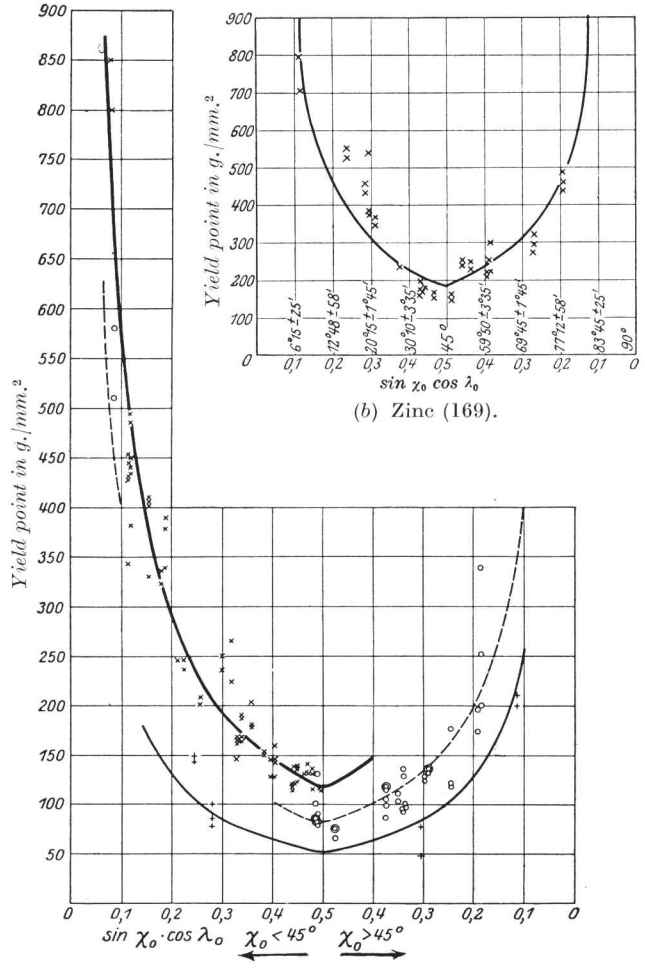

(*b*) Zinc (169).

(*c*) Cadmium (170). In this case the three groups of crystals investigated were drawn from the melt at various speeds (cf. Section 42).

FIG. 81 (*a*)–(*c*).—The Yield Point of Hexagonal Metal Crystals as a Function of Orientation.

Quantitative investigations on metal crystals of lower symmetry are available only for bismuth (177) and tin (178). These tests, too.

confirm the existence of a definite yield point characterized by a constant value of the critical shear stress in the operative glide system.

Since the Critical Shear Stress Law has so far been found consistently applicable, it is tempting to use it for the determination of slip elements that are still unknown. A comparison of the dependence of yield point on orientation, as calculated on the basis of various assumptions regarding the glide system, with that obtained experimentally, can in some circumstances reveal a preference for certain glide elements.

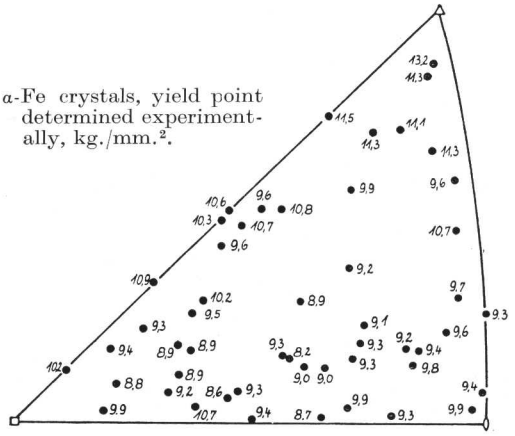

FIG. 82.—The Yield Point of Fe Crystals in Relation to Orientation (176).

In (179) the plasticity condition for crystals is described in an entirely different way from that outlined above. The yield condition is represented by a quadratic function of the principal normal and shearing stresses, which would attain a characteristic constant value at the yield point. However, the results obtained with cubic metal crystals appear to us to dispose of this mathematically attractive attempt at a solution, and to confirm the superiority of the Critical Shear Stress Law (180).

As already explained, the yield point is characterized by the start of *substantial* plastic extension. It does not reveal the true start of permanent deformation. In fact, it is certain that plastic extension can be observed at much lower stresses, and that its mechanism is identical with the glide which subsequently causes large deformations. Owing to the minute stresses involved, as well as to the very gradual start of deformation, an experimental determination of the actual beginning of plasticity is very difficult. Nevertheless, tests carried out on zinc crystals with the filament-extension apparatus showed that even at a plasticity limit corresponding to a permanent set of approximately 0·002 per cent., an approximately constant shear stress was found whose value was

less than half of that at the yield point (181). Moreover, tests carried out with the Martens apparatus on the elastic limit (0·001 per cent. permanent set) of aluminium crystals (182) indicate an approximately constant shear stress in the operative octahedral glide system (183). Furthermore, the recording of the first part of the stress–strain curve by precision measurement has shown that the section of the crystal is not without influence, inasmuch as with increasing diameter of the crystal the shear stress needed to produce a given amount of glide diminishes. This influence largely disappears within the limits of ordinary measurements (184).

41. *Torsion of Crystals*

Results are available of quantitative tests which have been carried out to determine the start of plastic torsion in crystals. A heat-treated copper–aluminium alloy (5 per cent. Cu) was used (185). In this case, too, a very marked dependence on orientation was observed. It would, therefore, seem advisable to resolve the applied stress into components with respect to the relevant octahedral glide systems.

In the first place it will be necessary to calculate, for a given torque (M), the shear and normal stresses (S and N) in a glide system (186). Let χ and λ again represent the angles between glide plane (T) and glide direction (t) and the longitudinal direction, while r represents the radius of the cylindrical crystal. The tangential shear stress $\tau_{\max.}$, which acts at the surface in an element of the section, is represented by the equation :

$$\tau_{\max.} = \frac{2M}{\pi r^3} \quad . \quad . \quad . \quad . \quad . \quad (41/1)$$

The point at the surface in which the stress is resolved into components is made the origin of a rectangular system of co-ordinates, the z-axis of which runs parallel to the cylindrical axis, while the x-axis points radially outwards. In this co-ordinate system the stress components are as follows :

$$\sigma_x = \sigma_y = \sigma_z = 0$$
$$\tau_{xy} = \tau_{zx} = 0$$
$$\tau_{yz} = \tau_{\max.} = \frac{2M}{\pi r^3}.$$

The glide direction and the normal to the glide plane are in this system given by the angles λ or $90 - \chi$ with the z-axis and the angles ψ_t or ψ_T between the x-axis and the projection of t, or of the

normal to T, on to the xy-plane. The condition for t to lie in T (*i.e.*, to be perpendicular to the normal of the glide plane) is expressed by the equation :

$$tg\chi = -\,tg\lambda \,.\, \cos(\psi_t - \psi_T) \quad . \quad . \quad . \quad (41/2)$$

In order to calculate the stress components with reference to the glide system, the system of co-ordinates is transformed into a new one, the z'-axis of which coincides with the normal of the glide plane,

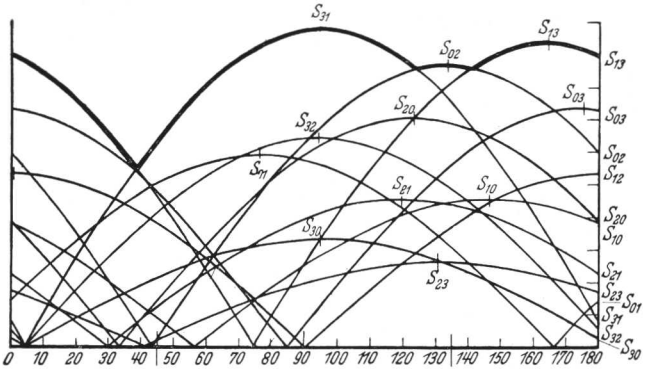

FIG. 83.—Torsion of an Aluminium Crystal. Relative Shear Stress in the 12 Octahedral Glide Systems along the Circumference of the Bar (186).

while the y'-axis coincides with the glide direction. $\sigma_{z'}$, and $\tau_{y'z'}$ are then the components required. They are given by :

$$\sigma_{z'} = \tau_{\max.} \,.\, \sin^2\chi \sin\psi_T \quad . \quad . \quad . \quad (41/3)$$

$$\tau_{y'z'} = \tau_{\max.} \,.\, (\cos\chi \cos\lambda \sin\psi_T + \sin\chi \sin\lambda \sin\psi_t) \quad . \quad (41/4)$$

The normal stress varies according to a sine function along the circumference of the crystal cylinder. A similar dependence holds also for the shear stress in the glide system, as is seen if ψ_t in formula (41/4) is eliminated by using equation (41/2). Fig. 83 shows an example for the variation of the shear stress in the twelve glide systems of an aluminium crystal.

Several series of tests on crystals of aluminium (186), silver (187), iron (188) and zinc (189) have shown that under torsional stress (alternating torsion) the operative glide system is the one that is exposed to maximum shear stress. In the work mentioned at the outset (185) the question has also been discussed whether, in addition, a torsional yield point characterized by a constant critical shear stress ($S_0 = \tau_{y'z'}$) in the operative system exists. The dependence

of the torque upon the orientation at such a yield point (186, 190) is given by :

$$M = \frac{\pi}{2} r^3 \tau_{\max.} =$$

$$\frac{\pi}{2} r^3 \frac{S_0}{\sqrt{\cos^2 \chi \cos^2 \lambda + \sin^2 \chi \sin^2 \lambda - 2 \sin^2 \chi \cos^2 \lambda}} \quad . \quad (41/5)$$

In the case of cubic face-centred crystals (octahedral glide) the extreme values of M are as follows :

$$M_{\min.} = \frac{\pi}{2} r^3 S_0$$

for $\chi = \lambda = 0$, *i.e.*, [110] is parallel to the longitudinal axis and
$\chi = \lambda = 90°$, *i.e.*, [111] is parallel to the longitudinal axis,

$$M_{\max.} = \frac{\pi}{2} r^3 S_0 \frac{1}{0{\cdot}577} = 1{\cdot}73 M_{\min.}$$

for $\chi = 35° 16'$, $\lambda = 90°$ *i.e.*, [100] parallel to the longitudinal axis.

The maximum torque at the yield point should therefore occur in crystals whose longitudinal direction is parallel to the cube edge ; it should exceed by 73 per cent. the torque valid for orientations parallel to the face or body diagonal.

The behaviour thus calculated theoretically on the basis of a constant critical shear stress was, in fact, approximately confirmed by experiments (cf. Fig. 84, which represents $\tau_{\max.}$ for a shear strain of 0·2 per cent.). It is true that the dependence on orientation revealed by the tests is more pronounced than that deduced from theory.

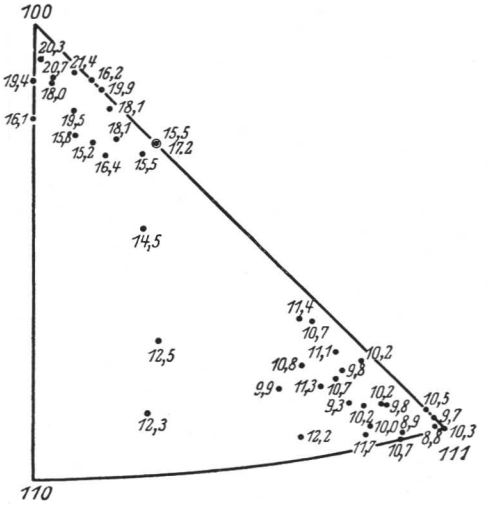

FIG. 84.—The Torsional Yield Point of Al Crystals (with 5% Cu) in Relation to Orientation (in kg./mm.²) (185).

The torsional yield point for the cube-edge orientation is 2·2 times greater than for the body diagonal orientation. In order to explain this difference it was assumed that plastic torsion begins not only in those parts of the crystal whose orientation to the applied stress is the most favourable, but simultaneously in the whole surface layer. A diagram of the "mean plastic resistance" of a thin-walled crystal tube in relation to the orientation of its longitudinal axis is found in Fig. 85. It will be noticed that on this assumption a better agreement with the experimental result is obtained. Even so, the theoretical dependence on orientation still falls somewhat short of the observed dependence.

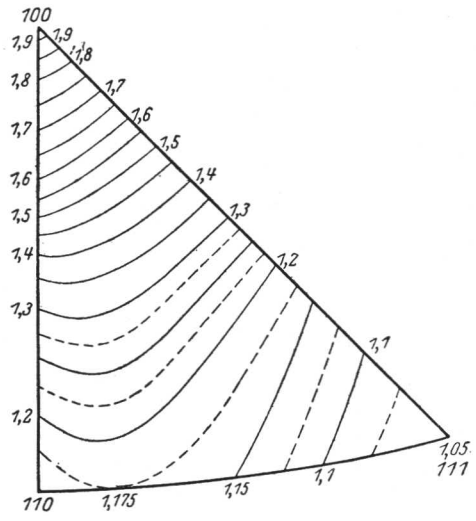

FIG. 85.—The "Mean Plastic Resistance", against Torsion, of an Al Crystal Tube, in Relation to Orientation (185).

The value of the critical shear stress in the torsional test (9–11 kg./mm.^{2}) approximates closely to the value of 9·0 kg./mm.^{2} obtained with the same crystal material in the tensile test.

If crystals (aluminium) are subjected to substantial torsion very characteristic changes in shape occur (191): these, too, depend on the orientation of the crystal; but they have not been investigated in detail so far.

42. *Critical Shear Stress of Metal Crystals*

Table IX gives a summary of the values so far measured of the critical shear stress of the principal glide systems of pure metals.

The figures, which are always of the order of approximately 100 g./mm.^{2} (corresponding to a yield point of the crystal, with the glide system at 45°, of approximately 200 g./mm.^{2}), reveal how very slight is the resistance of pure metals to deformation [cf. in this connection Section 45 and (192*a*)].

The table includes also, for the non-cubic metals, the elastic shear at the yield point parallel to the glide elements. In every case it is of the order of 10^{-5}. The significance of these minute values in the theoretical understanding of crystal plasticity will be discussed in Section 74. The shear is calculated with the aid of the equations

TABLE IX

Critical Shear Stress of Metal Crystals

Metal.	Purity of the initial material.	Method of production of crystal.	Glide elements.		Critical shear stress at the yield point, kg./mm.².	Shear modulus kg./mm.².	Elastic shear at the yield point.	Literature.
			T.	*t.*				
Copper	>99·9	Solidified in vacuo.	(111)	[101]	0·10	—	—	(174)
Silver	99·99				0·060			
Gold	99·99				0·092			
Nickel	99·8				0·58	—	—	(175)
Magnesium	99·95	Recrystallization.	(0001)	[11$\bar{2}$0]	0·083	1700	$4{\cdot}9_5 . 10^{-5}$	(168)
Zinc	99·96*	Drawn from the melt.	—	—	0·094	4080	2·3	(169)
Cadmium	99·996*		—	—	0·058	1730	$3{\cdot}3_5$	(170)
β-Tin	99·99*		(100)	[001]	0·189	1790	10·6	(178)
			(110)		0·133	1790	$7{\cdot}4_3$	
Bismuth	99·9*		(111)	[10$\bar{1}$]	0·221	970	22·8	(177)

* "Kahlbaum" Brand.

(7/2). These equations, which refer to the principal crystallographic system of co-ordinates, must, for the present purpose, be transformed to a system in which the z-axis is placed at right angles to the operative glide plane, while the y-axis coincides with the direction of glide. γ_{yz} is then the required elastic shear in the glide system. The six stress components occurring in the expression for γ_{yz}, if σ is the applied tensile stress and χ and λ the angles between tensile direction and the elements, are given by :

$$\begin{aligned} \sigma_x &= \sigma . (\sin^2\lambda - \sin^2\chi); & \tau_{yz} &= \sigma . \sin\chi\cos\lambda \\ \sigma_y &= \sigma . \cos^2\lambda & \tau_{zx} &= \sigma . \sin\chi \sqrt{\sin^2\lambda - \sin^2\chi} \\ \sigma_z &= \sigma . \sin^2\chi & \tau_{xy} &= \sigma . \cos\lambda \sqrt{\sin^2\lambda - \sin^2\chi} \end{aligned} \qquad (42/1)$$

The transformation of the modulus of elasticity (s_{ik}) from the principal crystallographic system of co-ordinates to the new co-ordinate system (s'_{ik}) proceeds according to the usual transformation formulæ (192).

If these calculations are carried out for the crystal types and glide

systems contained in Table X [1] (180), it is found that five of the six elasticity coefficients disappear and that only s'_{44} differs from zero. This means that in all such cases the shear γ_{yz} in the glide system is proportional to the shear stress τ_{yz}. Constancy of shear stress and constancy of shear strain are therefore identical conditions. It

TABLE X

Shear Coefficient s'_{44} in the Glide System

Lattice type.	Crystal class.	Glide elements.		s'_{44}.
		T.	*t.*	
NaCl lattice	O_h	(101)	[10$\bar{1}$]	$2\,(s_{11} - s_{12})$
Hexagonal close-packed . .	D_{6h}	(0001)	[11$\bar{2}$0]	s_{44}
Tetragonal (β-tin) . . .	D_{4h}	(100) (110)	[001] [001]	s_{44} s_{44}
Rhombohedral . . .	D_{3d}	(111)	[101]	s_{44}

naturally follows that the elastic energy of shear at the yield point is also a constant independent of orientation; it amounts to 10^{-6} cal./g. for the pure metals listed in Table IX.

However, there is no proportionality between shear stress and shear strain for the octahedral glide of the cubic crystals. A decision between the conditions of constant shear stress or constant shear strain at the yield point can therefore be made as a result of tests with cubic face-centred metal crystals. Shear in this case is calculated by :

$$\gamma_{yz} = \left[\frac{4}{3}(s_{11} - s_{12}) + \frac{1}{3}s_{44}\right] \cdot \tau_{yz} + \frac{\sqrt{2}}{3}[s_{44} - 2(s_{11} - s_{12})] \cdot \tau_{xy} \,. \quad (42/2)$$

Significant deviations from the proportionality between shear stress and shear strain occur only when the second term of the expression for γ_{yz} can no longer be neglected beside the first. This is the case with crystals of a decidedly anisotropic character [isotropy is represented by $s_{44} = 2(s_{11} - s_{12})$], and with crystals having orientation areas in which λ is much greater than χ (marked deviation of the direction of glide from the projection of the tensile direction on the glide plane).

[1] In addition to the glide of metal crystals the table contains particulars of the dodecahedral glide of cubic crystals of the rock salt type.

The average errors of the mean values of shear stress and shear strain for the four examples in which the dependence of yield point on orientation has been examined, are collected in Table XI. For

TABLE XI

Mean Shear Stress and Shear Strain at the Yield Point of Cubic Face-centred Metal Crystals with Octahedral Glide

Metal.	Critical shear stress, kg./mm.².	Elastic shear strain.	Degree of anisotropy $s_{44} - 2(s_{11} - s_{12})$ cm.²/Dyn.
Silver (174) .	0·060 ± 5·8%	$2{\cdot}69 \cdot 10^{-5} \pm 8{\cdot}5\%$	$-43{\cdot}4 \cdot 10^{-13}$
Gold (174) .	0·092 ± 2·4%	$4{\cdot}12 \cdot 10^{-5} \pm 7{\cdot}0\%$	$-43{\cdot}2 \cdot 10^{-13}$
α-Brass (173) .	1·44 ± 1·9%	$43{\cdot}3 \cdot 10^{-5} \pm 10{\cdot}8\%$	$-41{\cdot}6 \cdot 10^{-13}$
Al–Cu alloy (age-hardened) (172)	9·2 ± 2·1%	$355 \cdot 10^{-5} \pm 2{\cdot}0\%$	$-6{\cdot}8 \cdot 10^{-13}$

the elastically anisotropic metals, silver, gold, α-brass, the difference between the mean errors is considerable : the mean error for the shear strain always exceeds substantially that for the shear stress. In the case of the practically isotropic aluminium there is no difference. This table would therefore appear to justify the assumption that it is constancy of shear stress and not constancy of elastic shear that characterizes the yield point for crystal glide.

The numerical value of the critical shear stress depends in a very marked degree on various circumstances. We shall deal in subsequent sections with the importance of impurities (alloying), temperature, speed of deformation and mechanical pre-working. At present we shall discuss, briefly, the influence of the method of production, the speed of growth during formation of crystals, and annealing.

Magnesium crystals that had been drawn from the melt, and which contained the same impurities as the recrystallized crystals mentioned in Table IX, had an appreciably higher critical shear stress than these, amounting to 103·3 g./mm.² (193). Table XII contains the critical shear stress of *cadmium* crystals drawn from the melt at varying speeds : the slower the rate of crystal growth, the lower the shear stress.[1] Subsequent heat treatment can also greatly reduce

[1] Zinc crystals behave in a similar manner (194).

the yield stress of the basal plane if the crystal has been drawn quickly from the melt. Annealing at an elevated temperature (300° C.), on the other hand, causes an increase in the critical shear

TABLE XII

Influence of the Speed of Withdrawal from the Melt and of Annealing on the Critical Shear Stress of Cadmium Crystals (170)

Speed of withdrawal.	Critical shear stress.	Heat treatment of crystals drawn from the melt at the rate of 20 cm./hour.		Critical shear stress.
20 cm./hour	58·4 g./mm.²	0 hours	275° C.	58·4 g./mm.²
5–10 ,,	39·7 ,,	16 ,,	275° C.	43·5 ,,
1·5 ,,	25·5 ,,	24 ,,	275° C.	27·4 ,,

stress with increasing duration of the heat treatment, amounting to approximately 75 per cent. after 6 hours' treatment. It would appear that this phenomenon could be explained by crystal recovery (Section 49) or by the temperature dependence of the solubility of impurities (195).

The critical shear stresses contained in Table IX relate to the *principal glide system*, at room temperature, of the metal crystal

TABLE XIII

Critical Shear Stress and Closeness of Packing of the Glide Elements of Tin Crystals (178)

Glide system.		Critical shear stress, g./mm.².	Closeness of packing.		Spacing of the lattice planes from T, Å.
T.	t.		T.	t.	
(100)	[001]	189	1	1	2·91
(110)	[001]	133	0·706	1	2·06
(101)	[10$\bar{1}$]	160	0·478	0·478	2·09 and 0·70
(121)	[10$\bar{1}$]	170	0·346	0·478	1·84 ,, 0·61

concerned. The yield stresses of the next best glide systems (crystallographically non-equivalent) have so far only been determined quantitatively for the tin crystal (Table XIII). In four crystallographically different glide systems the critical shear stresses

differ only slightly. The relationship between capacity for glide and closeness of packing, which was mentioned earlier and found to have been more or less confirmed, is now revealed by the example of tin to be only a rough approximation. Only the lower limits of the critical stress can be given for the further glide systems of other crystals. For instance, these can be deduced from the orientation range in which the main glide system remains operative. Thus the critical stress of the pyramidal plane type I order 1 of the cadmium crystal (which, however, has not yet been observed as a glide plane) is at least 4·7 times that of the basal plane. When we come to discuss, in Section 48, the question of extension at elevated temperatures, we shall be in a position to assess more accurately the capacity for glide of the second-best glide system, using the aluminium crystal as an example.

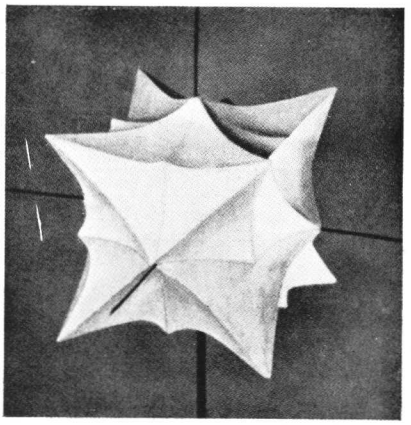

FIG. 86.—Plastic Yield Surface of Cubic Crystals with Octahedral Glide (183).

A graphical representation of the dependence of the yield point of crystals on their orientation, as deduced from the Shear Stress Law, can now be given in two figures. Fig. 86 illustrates the plastic yield surface of cubic crystals with octahedral glide (or dodecahedral glide with the body diagonal as glide direction). The radius vector from the centre of the solid is a measure of the magnitude of the yield point in the direction concerned. The model illustrates clearly the way in which resistance to plastic deformation depends upon direction. The minimum yield point values occur in directions which include the angles 20° 46′, 65° 52′ and 84° 44′ with the three axes of the cube (glide plane and glide direction are in this case at 45° to the direction of stress); the maximum yield point lies on the body diagonals. The ratio of the yield point of the strongest crystal to that of the weakest amounts to 1·84.

An example of the dependence of the yield point on the orientation of hexagonal crystals with basal glide is given in Fig. 87, which represents a section through the plastic-yield

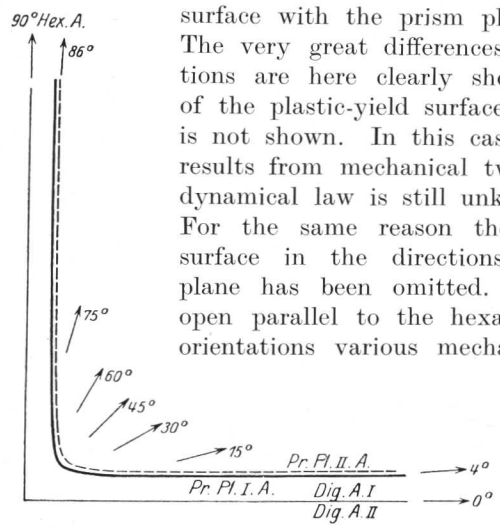

FIG. 87.—Sections through the Plastic Yield Surface of Hexagonal Crystals with Basal Glide (170).

surface with the prism planes types I and II. The very great differences in the various directions are here clearly shown. The intersection of the plastic-yield surface with the basal plane is not shown. In this case, plastic deformation results from mechanical twinning, for which the dynamical law is still unknown (cf. Section 51). For the same reason the termination of the surface in the directions lying in the basal plane has been omitted. The surface is also open parallel to the hexagonal axis. For such orientations various mechanisms become operative with the individual metals (twinning with magnesium, basal cleavage with zinc, pyramidal glide with cadmium).

43. *The Progress of Glide. The Yield–Stress*[1] *Curve*

Having established that the yield point of magnesium is bound up with the attainment of a definite shear stress in the glide system, the question now arises whether this shear stress is operative for the further course of extension, or whether the shear stress in the glide system changes with increasing deformation. A direct answer to this question is supplied by a comparison of stress–strain curves obtained experimentally, with curves calculated on the assumption that the shear stress in the operative glide system is constant (196). This calculation is as follows. In first place the equation (40/1) gives

$$\sigma = \frac{S_0}{\sin \chi_0 \cos \lambda_0}.$$

$\frac{1}{\sin \chi_0}$ represents the area of a glide which remains constant during

[1] *Footnote of Translator.* " Yield point " is according to the preceding sections the stress at which substantial plastic deformation begins *in a previously undeformed* crystal. " Yield stress " is the stress at which plastic deformation continues *in a previously deformed* crystal (or poly-crystalline specimen). The yield stress depends on the magnitude of the preceding strain; its value for the strain 0 is the yield point. In what follows " yield stress " will usually mean the resolved shear stress in the glide system at which plastic glide ontinues after a given glide strain.

extension. As a first approximation the *stressed* portion of the glide ellipse is also given by this expression, since the sickle-shaped area which becomes exposed in the course of glide is negligible compared with the total area. By means of the factor $\cos \lambda_0$ the components in the glide direction are obtained from the tensile stress. Owing to the lattice rotation which accompanies glide, this factor does not remain constant. Its variation is given by the extension formula (26/1), so that ultimately we obtain

$$\sigma = \frac{S_0}{\sin \chi_0} \cdot \frac{1}{\cos \lambda} = \frac{S_0}{\sin \chi_0} \cdot \frac{1}{\sqrt{1 - \frac{\sin^2 \lambda_0}{d^2}}} \quad . \quad . \quad (43/1)$$

This formula represents the equation of the stress–strain curve for

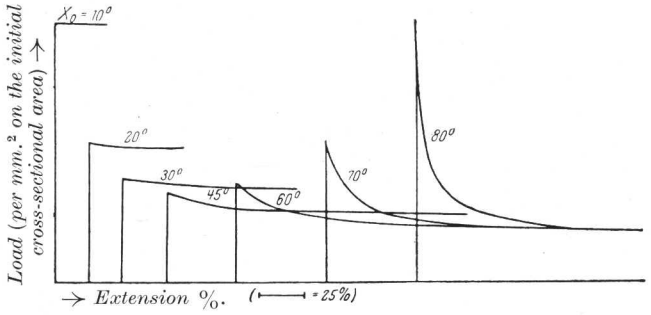

FIG. 88.—Theoretically Determined Stress–Strain Curves, Based on Constancy of the Shear Stress of the Glide System (197). ($\lambda_0 = \chi_0$ is assumed—a permissible simplification.)

various initial orientations of the glide elements given by angles χ_0 and λ_0. Fig. 88 contains these theoretical stress–strain curves, characterized by constancy of shear stress, for a number of orientations. It will be observed that *in all cases* extension takes place at a continuously falling stress; the more transverse the original position of the glide elements in the crystal, the greater the drop of stress.

The stress–strain curves in Fig. 89 which were obtained experimentally on cadmium crystals, reveal once more the great importance of the initial position of the glide elements; the energy of deformation necessary to obtain a given amount of extension (area below the curve) is very dependent on the orientation. In addition, the curves show that in most cases the stress *increases* appreciably in the course of extension. It is true that, where the initial position

of the basal plane is transverse, a drop of stress can be observed, but here, too, the stress increases again as extension proceeds. A comparison of Figs. 88 and 89, therefore, reveals that when cadmium crystals are stretched the shear stress in the operative glide system remains by no means constant, but increases substantially with increasing deformation.

These two observations (exemplified by cadmium crystals), namely, that the shape of the curve depends on orientation, and that the operative shear stress increases with increasing deformation, have been confirmed by all stress–strain curves obtained with other metals. We meet here for the first time the technologically important phenomenon of the *work-hardening* of metal crystals by plastic

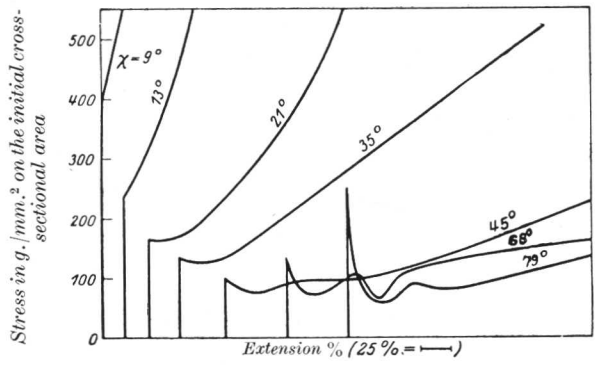

FIG. 89.—Experimental Stress–Strain Curves of Cd Crystals (170).

deformation [(198), (199)]. Moreover, it is a question of shear-hardening, as expressed by an increase, in the operative glide system, of the shear stress needed for further deformation.

Before embarking upon a detailed analysis of the stress–strain curves two observations should be made. The first refers to certain *discontinuities* in the *course of extension*. It was found that zinc crystals, especially after previous deformation by bending backwards and forwards, stretched in a series of regular jumps, so long as extension was confined to the lower range (200). The magnitude of the jumps was about 1 μ. With very pure zinc crystals (99·998 per cent.) this stepwise deformation was also observed in the normal tensile test (201). The magnitude of the jumps depends in a large measure upon the orientation of the crystal. While there are no discontinuities if the glide elements are in an oblique position, they have been observed to amount to as much as 80 μ where the glide

plane was more transverse. The fact that the jumps also occur when the surface of the crystal is dissolved during extension shows that they are not due to a surface effect. The phenomenon disappears at a temperature of −185° C. Common to all cases of markedly jerky glide is the fact that they occur within a range of the stress–strain curve where the stress is falling, or at least stationary. An oblique initial position of the glide plane, reduction of the

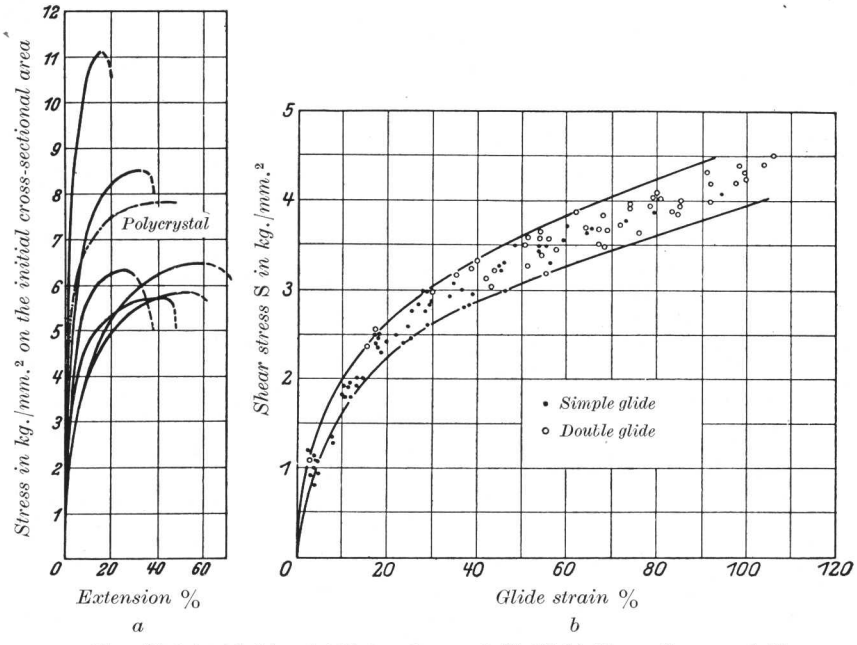

FIG. 90 (*a*) and (*b*).—(*a*) Extension, and (*b*) Yield–Stress Curves of Al Crystals (203).

temperature and substantial deformation, all of which lead to a relatively steep *increase* of the stress, prevent jerky extension. On the other hand, a decrease of stress accompanying increasing deformation is not a sufficient condition for the occurrence of jerky glide. This is shown by cadmium (or tin) crystals which, in spite of exceptionally large reductions in load, exhibit only very small jumps at the onset of stretch.

The second observation relates to *local contractions* (necking) which occur with crystals of oblique orientations at the start of extension (Figs. 79 and 121). In this case, owing to the initial

decrease in stress, the extension is limited at the outset to those portions of the crystal which are first deformed; not until extension has proceeded further does the entire length of the crystal participate in the deformation. However, where there has been only slight hardening it may happen that the extension will not spread and that fracture will result from continued glide at the first contraction (202) (cf. also Fig. 123). If the glide elements are initially in an

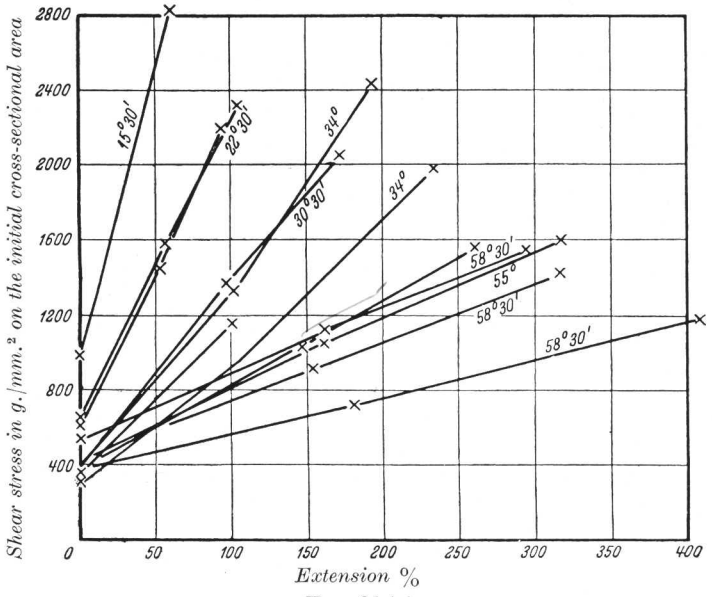

Fig. 91 (*a*)

oblique position, the crystal will as a rule stretch uniformly from the start.

Having ascertained that the stress–strain curve of metal crystals, like their yield point, depends on the position of the glide elements, we must now enquire whether this curve cannot be explained in terms of orientation, in the same way as the yield point was related to the critical shear stress. Obviously, it will be useful to employ co-ordinates which express the process of glide more adequately than do extension and stress. Suitable "crystallographic" co-ordinates for this purpose have been found in the glide strain and in the resolved shear stress in the glide system [(203), (204)], with which we have already dealt in Section 26. One arrives in this way at a method by which the whole set of the stress–strain curves for

various orientations can be satisfactorily represented by a *single* curve, the " yield–stress " curve. The extension and the yield–

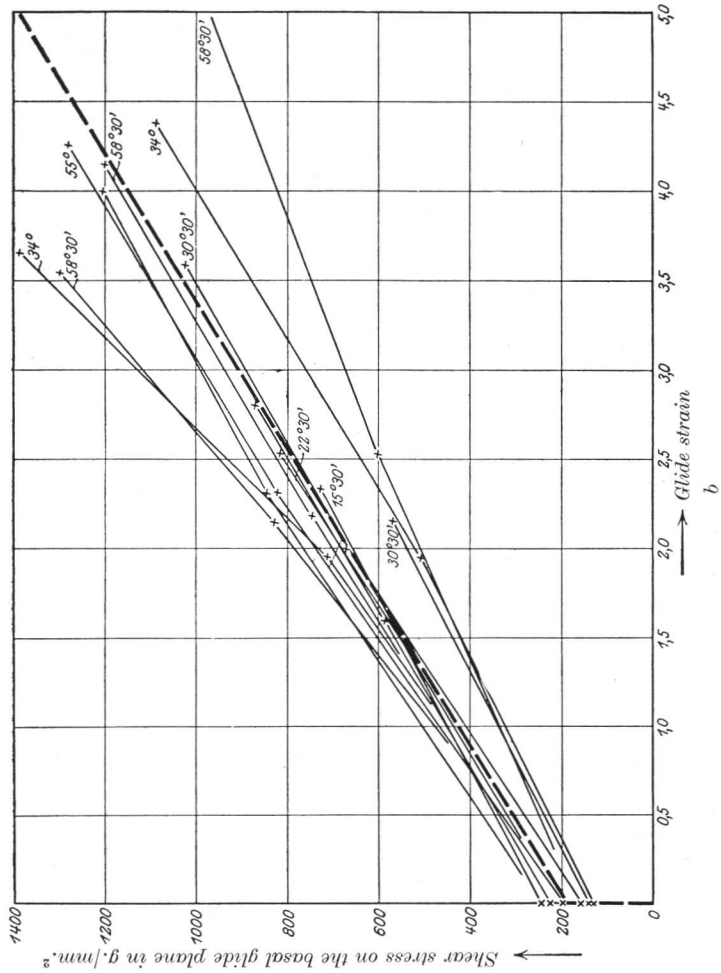

FIG. 91 (*a*) and (*b*).—(*a*) Extension and (*b*) Yield–Stress Curves of Zn Crystals (204). The Initial Angle of the Basal Plane (χ_0) is Indicated in Each Case.

stress curves of aluminium and zinc crystals of various orientations shown in Figs. 90 and 91, may serve as an example.[1] The shear

[1] The calculation of the shear stress from stress, extension and initial position of the glide elements is readily obtained by solving the equation (43/1) with respect to S : $S = \sigma \,.\, \sin \chi_0 \sqrt{1 - \frac{\sin^2 \lambda_0}{d^2}}$.

The glide strain is calculated according to the formula (26/3).

stress of the operative glide system continues therefore to be independent of the normal stress *during* glide. This is most impressively demonstrated in the case of aluminium crystals (Fig. 92), for which the yield–stress curves in compression (where the normal stress in the glide plane is compressive) coincide with those from the tensile tests (where the normal stress is *tensile*). As will be seen from Fig. 90 the yield stress continues without a break even after double glide starts.

Systematic deviations from the mean curve occur with cubic crystals only for initial orientations in which more than two glide systems are almost equally favoured, and in which, consequently,

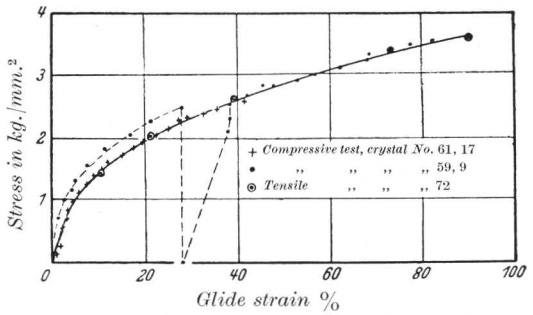

FIG. 92.—Tensile and Compressive Shear–Stress Curves of Al Crystals (205).

Orientation of the crystals : 61, 17: $\chi_0 = 44°$ $\lambda_0 = 46{\cdot}5°$
59, 9 $33°$ $35{\cdot}2°$
72 $48{\cdot}1°$ $52{\cdot}1°$

disturbances in the progress of extension may be expected. In the case of hexagonal metal crystals the scatter of the individual curves about the mean curve is to some extent due to the formation of twins—a phenomenon to which we shall refer later.

A summary of the yield–stress curves obtained hitherto with crystals of pure metals is given in Fig. 93. The substantially better glide capacity of the single-glide system of hexagonal crystals and of the principal glide systems of the tetragonal tin is very clear.[1]

The yield–stress curve describes the increase in the shear stress of the glide system that is operative in extensions. Close observation of the lattice rotation in the course of stretching gives an indication of the magnitude of the shear hardening in crystallographically equivalent latent glide systems. If the lattice rotation correspond-

[1] An attempt has been made in (214) to explain, in terms of atomic displacements, this striking difference in the behaviour of crystals of the two closest-packed systems.

ing to the new system occurs *before* the achievement of a geometrically equally favourable position, then this system has become less hardened than the operative one; if, on the other hand, while the first system is exclusively operated, the symmetrical position is *exceeded*, then the latent system has become *more* hardened.

The results obtained with cubic metals (aluminium, nickel, copper, silver, gold) indicate that the second glide system always begins to operate when the symmetrical position has been either reached or

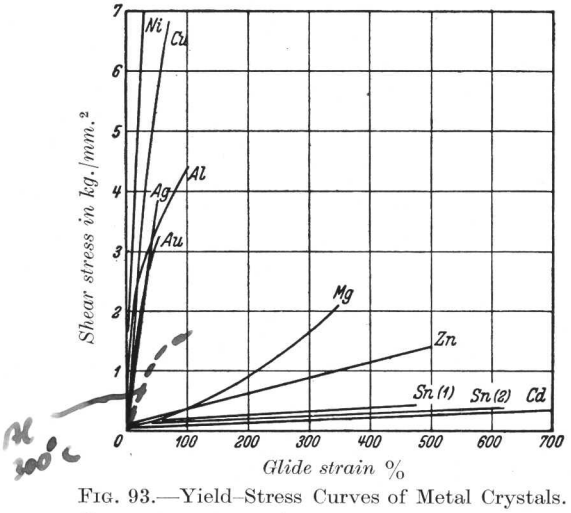

FIG. 93.—Yield–Stress Curves of Metal Crystals.

Cu (207); see also (206, 208)		Mg (210)
Ag (207)		Zn (211)
Au (207)		Cd (212)
Al (209)	Sn (1): $T = (100)$; $t = [001]$	(213)
Ni (208)	Sn (2): $T = (110)$; $t = [001]$	

only slightly exceeded (cf. Figs. 62 and 63). This means that in such cases the latent octahedral glide system becomes as hardened as, or even slightly more hardened than, the operative system [(215), (216)]. In the case of tin crystals the end position which is sometimes observed with crystals stretched in a [101] direction indicates that a latent glide system with $T = (101)$ $t = [10\bar{1}]$ hardens *substantially* more than the crystallographically equivalent system. No details are yet available regarding the hardening of crystallographically *non-equivalent* latent glide systems.

Attempts have often been made to express the yield–stress curve by an equation. With such an equation, which represents S as a function of a and hence of d, the dependence of the usual stress–

strain curves on orientation could be mathematically represented by substituting it for S_0 in (43/1). For the linear increase of the shear stress, which is often approximately valid for hexagonal metals :

$$(S = S_0 + ka) \quad . \quad . \quad . \quad . \quad . \quad (43/2)$$

there results (197)

$$\sigma = \frac{d}{\sin^2 \chi_0}\left(k + \frac{S_0 \sin \chi_0 - k \cos \lambda_0}{\sqrt{d^2 - \sin^2 \lambda_0}}\right) \quad . \quad . \quad (43/3)$$

k, the tangent of the angle of inclination of the yield–stress curve, becomes the coefficient of hardening.

The yield–stress curve for aluminium crystals shown in Fig. 90 is expressed approximately by the equation (217)

$$S = 4{\cdot}2_8 a^{0,33} \quad . \quad . \quad . \quad . \quad . \quad (43/4)$$

Other formal representations of the yield–stress curve of aluminium crystals will be found in (218), (219) and especially in (220), which also contains a theoretical foundation (cf. Section 76).

44. *Termination of Glide*

Such simple and general principles as the Critical Shear Stress Law and the yield–stress curve, which govern the inception or progress of glide, do not hold for its conclusion, since very diverse processes may bring this about. We will discuss in the first place the relatively simple behaviour of the hexagonal metals, and afterwards that of the cubic metals, where rupture is accompanied by necking.

With magnesium crystals glide terminates with the fracture of the crystal, the fracture occurring variously according to the orientation of the basal plane to the direction of tension. Where the initial angle is greater than $\sim 12°$ a shear fracture showing a stepped surface occurs in the basal slip plane ; as a result of the steps the surface of fracture lies more obliquely than the basal plane in the crystal (Fig. 94). Where the basal plane of the crystal is very oblique, the fracture either passes more or less transversely through the crystal or it follows a twin plane. With zinc and cadmium crystals the basal glide is limited at room temperature solely by the operation of the second crystallographic mechanism of deformation : mechanical twinning. In both cases deformation twins are formed on a $(10\bar{1}2)$ plane ; a new secondary basal glide develops in the twins which, accompanied by a drop of load, leads to a marked necking of the crystal ribbon and to final rupture (cf. Fig. 73 ; for further details see Section 52).

With these crystals and the magnesium crystal, which fails by a shear fracture, the primary basal glide generally comes to an end when a limiting shear stress characteristic of the metal is reached in the glide system. This statement, however, applies only to such crystals where the basal plane was originally at an angle of more

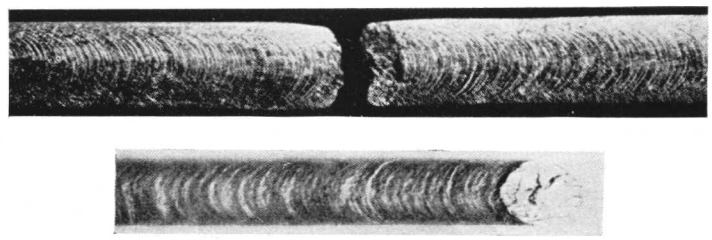

FIG. 94.—Fracture of Magnesium Crystals [(221), (210)].

than 15–20° to the longitudinal direction. It is based not only on experiments at room temperature, but also on a number of experiments designed to test the relationship between crystal plasticity and temperature (Section 48).

Consequently it is not only the start (yield point) and the slope (coefficient of hardening) which are characteristic for the yield–

TABLE XIV

Conclusion of the Basal Glide of Hexagonal Metal Crystals

Metal.	Shear strength of the basal plane in g./mm.².		Upper limit of glide strain, %.	Work of deformation, cal./g.
	at the start of glide.	at the conclusion of glide.		
Magnesium (210) .	83	2100	350	4·09
Zinc (222) . .	73	1220	380	0·84
Cadmium (223) .	58	420	500	0·26

stress curve of these hexagonal crystals : the conclusion of the curve is also substantially independent of crystal orientation over a wide range. Therefore the upper limit of the glide strain and the work of deformation (the surface below the yield–stress curve) are likewise constants independent of orientation. The relevant values at room temperature for magnesium, zinc and cadmium will be found in Table XIV.

On the basis of these values it is now possible, by a simple calculation, to arrive at the dependence of final orientation, maximum load

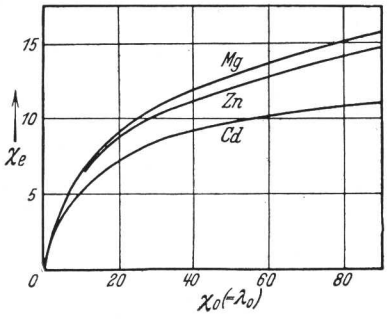

FIG. 95.—Final Angle of the Basal Plane as a Function of its Initial Angle in the Extension of Hexagonal Crystals.

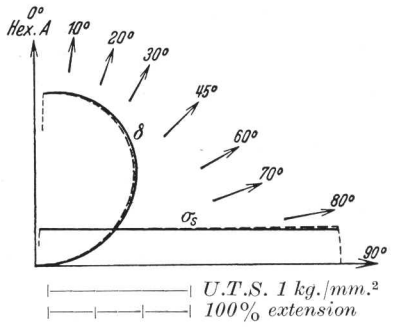

FIG. 96.—Sections of the Ultimate Tensile Stress and Extension Surface of Zn Crystals with Prism-plane Type I (Continuous Line) and Prism Type II (Discontinuous Line) (224).

and extension, upon the initial position of the lattice. Assuming for the sake of simplicity that $\lambda_0 = \chi_0$ (this does not substantially impair the generality) then formula 26/4*a* gives the values shown in Fig. 95 for the final angle of the basal plane. These correspond substantially with experimental results. The extension is derived from the initial and the final orientation according to the extension formulæ (26/1, 2), while the maximum load per square millimetre of the initial cross-section (the ultimate tensile stress) is obtained by inserting the limiting shear stress S_e in the equation (43/1). Fig. 96 gives as an example sections of the extension and ultimate tensile-stress surface of zinc crystals; while Fig. 97 represents a model of the extension surface (cadmium).

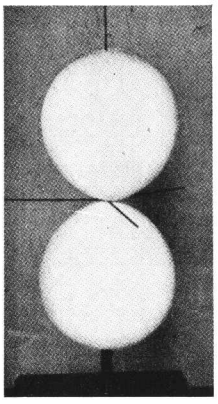

FIG. 97.—Model of the Extension Surface of Cd (212).

The true stress corresponding to the maximum load, unlike the ultimate tensile stress, is substantially independent of the initial orientation, owing to the constant final shear stress of the basal plane and to the very similar final orientations of stretched crystals.

We shall discuss in Sections 53 and 54 the question of the termination of primary basal glide of zinc crystals by basal cleavage, which occurs at low temperatures.

The extension of *cubic* metal crystals is in no wise limited by a condition of constant final shear stress in the glide system, independent of orientation. In this case, double glide will always occur sooner or later in two crystallographically equivalent glide systems which are geometrically equally favourable, leading to necking and so finally to fracture. With such crystals the end of the uniform extension occurs when the maximum load has been reached, since necking itself is accompanied by a reduction of load. Table XV

TABLE XV

Ultimate Tensile Stress and Elongation of Cubic Metal Crystals

Metal.	Ultimate tensile stress, kg./mm.².	Elongation, %.
Aluminium (226) . . .	5·9–11·5	19–68
Copper (227)	12·9–35·0	10–55
α-Iron (228)	16–23	20–80
Tungsten (229)	105–120	—

shows the dependence of the ultimate tensile stress (as given by maximum load and initial section) and of the uniform extension on the orientation. In addition, Fig. 98 illustrates, with the aid of models, the experimental results of tensile tests on copper crystals of various orientations.

A mathematical determination of the maximum-load point can be attempted by differentiating the equation of the load–extension curves :

$$\sigma = f(d) = \frac{S(a)}{\sin \chi_0 \sqrt{1 - \frac{\sin^2 \lambda_0}{d^2}}}$$

with respect to the extension, and putting $\frac{d\sigma}{dd} = 0$ [cf. (43/1); $S(a)$ is the equation of the yield–stress curve of the operative glide system]. The following is then obtained :

$$\frac{dS}{da}_{\kappa} = S(a) \cdot \frac{\sin \chi_0 \sin^2 \lambda_0}{(\cos \lambda_0 + a \sin \chi_0)(1 + 2a \sin \chi_0 \cos \lambda_0 + a^2 \sin^2 \chi_0)}$$

If the equation of the yield–stress curve is known, this expression connects the glide strain which corresponds to the maximum tensile stress with the initial position of the glide elements. Whether the

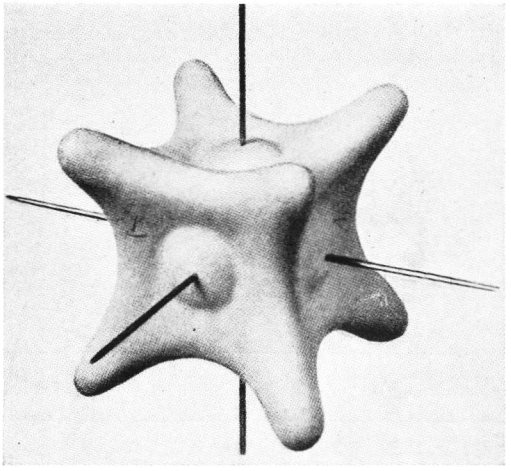

FIG. 98 *a*]

values determined in this manner really do correspond to a *maximum* of the extension curve, is seen from the sign of $\frac{d^2\sigma}{dd^2}$. For the extreme case we have

$$\frac{d^2\sigma}{dd^2} = \frac{d^2S}{da^2} \cdot \frac{1 + 2a \sin \chi_0 \cos \lambda_0 + a^2 \sin^2 \chi_0}{(\cos \lambda_0 + a \sin \chi_0)^2} +$$

$$+ 3S \cdot \frac{\sin^2 \chi_0 \sin^2 \lambda_0}{(\cos \lambda_0 + a \sin \chi_0)^2 (1 + 2a \sin \chi_0 \cos \lambda_0 + a^2 \sin^2 \chi_0)}$$

This expression, which in the case of a maximum load would have to be *negative*, has *always a positive* sign whenever the resolved shear stress increases linearly or with a higher power of the glide strain. In agreement with what is known of hexagonal crystals, a maximum load for such yield–stress curves can never be reached with simple glide; the extreme value obtained from $\frac{d\sigma}{dd} = 0$ represents a minimum in the extension curve. A maximum load can be reached only when the increase of the shear stress with the glide strain is less than linear.

But even in the cases of the yield–stress curve given above for aluminium crystals a maximum in the extension curve will not be reached with simple glide. On the other hand, a maximum load

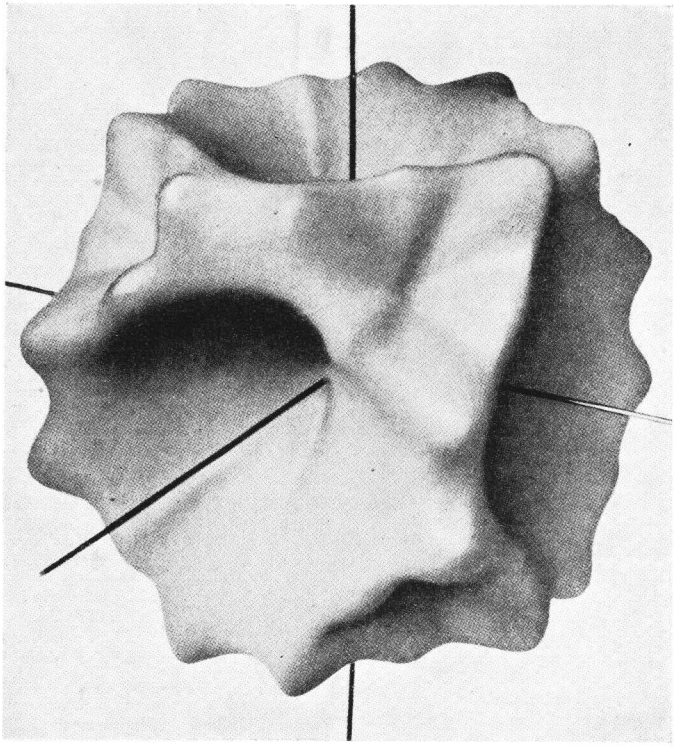

b

Fig. 98 (*a*) and (*b*).—(*a*) Ultimate Tensile Stress and (*b*) Extension Surfaces of Cu Crystals; as Determined Experimentally (225).

will be reached in the region of double glide. The result of the calculations, which cannot always be carried out exactly and which we do not propose to discuss here, is graphically represented by the ultimate tensile stress and extension surfaces of aluminium crystals shown in Fig. 99. In general, the results are satisfactorily confirmed by experience, although in the case of extension the discrepancies amount to as much as 50 per cent.

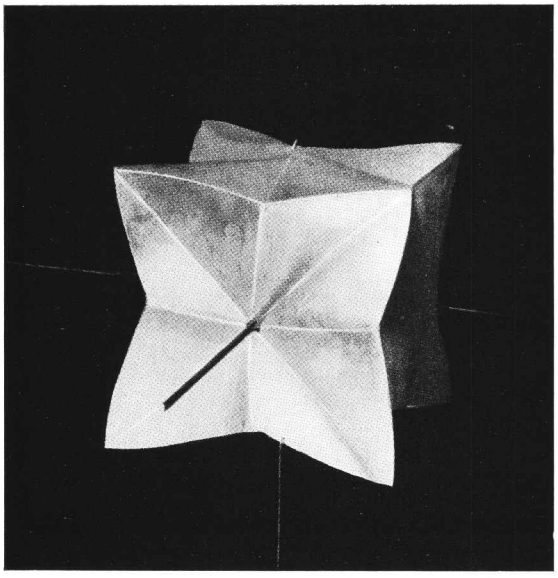

a

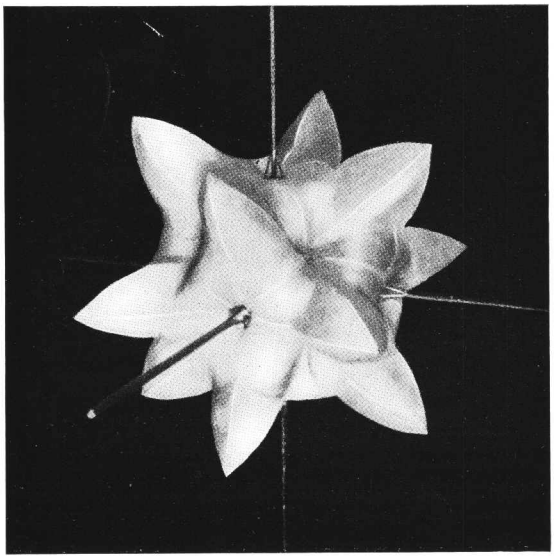

b

FIG. 99 (*a*) and (*b*).—(*a*) Ultimate Tensile Stress and (*b*) Extension Surfaces of Al Crystals; Calculated (217).

(*b*) EFFECT OF ALLOYING

Hitherto in dealing with the beginning, progress and termination of glide, we have confined our observations to the " pure " metals. In Table IX will be found the purity percentage of these metals. These materials do not afford a safe guide to the behaviour of *absolutely* pure metal crystals, since even very small impurities have an extraordinarily large effect. The influence of alloying on the plasticity of metal crystals will be described in the following two sections.

45. *The Start of Glide in Alloyed Metal Crystals*

The study of the initiation of glide in alloyed metal crystals is greatly facilitated by the observation, so far invariably made, that the yield point of such crystals is much more pronounced than that of similarly oriented crystals of the pure metal.

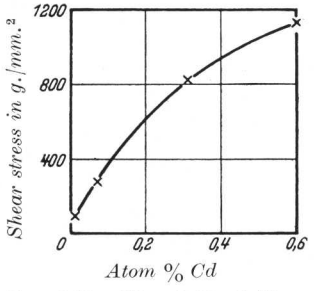

FIG. 100.—The Critical Shear Stress of Cd–Zn Solid Solutions as a Function of Concentration (230).

The example of the critical shear stress of *zinc* crystals alloyed with cadmium shows how strongly even small additions can influence the plastic behaviour of metal crystals (Fig. 100). A content of 0·60 atomic-per cent. cadmium (1·03 weight-per cent.) raises S_0 from the value of 94 g./mm.^{2} (for the " Kahlbaum " material with 0·03 weight-per cent. cadmium) to 1150 g./mm.^{2}—a more than twelve-fold increase.[1] Linear extrapolation to a cadmium content of 0 per cent. gives a shear stress of 40 g./mm.^{2} for the yield point of the cadmium-free zinc crystal—which, however, still contains traces of lead and iron. Recently this value was all but achieved (49 g./mm.^{2}) with crystal material produced from " Kahlbaum " zinc refined by distillation, the cadmium content of which was less than 5×10^{-4} atomic-per cent. (201).

Alloying has a much smaller hardening effect if the added element

[1] That cadmium was present in solution in the alloy crystals drawn from the melt was established by X-ray examination (244). We have here supersaturated solid solutions, since below 100° C. cadmium is practically insoluble in zinc.

forms a second phase in the matrix. Fig. 101 shows the polished section of a zinc crystal alloyed with 2 per cent. tin, in which layers of zinc–tin eutectic have come to lie parallel to the basal plane. The initial critical shear stress of the basal plane undergoes as a result no more than a four-fold increase.

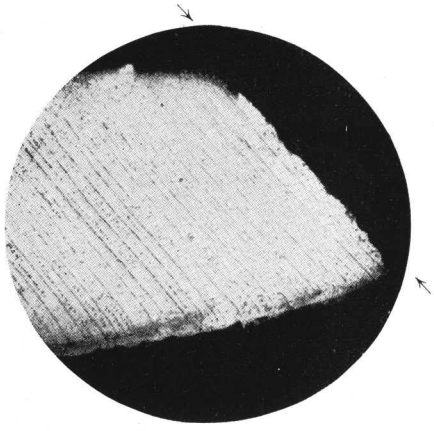

FIG. 101.—Polished Section of a Zn Crystal in which Zn–Sn Eutectic is Present (230).

Fig. 102 relates to the binary solid solution systems of aluminium–magnesium and zinc–magnesium. It gives the hardening ($v_{\text{all.}}$) due to alloying as a function of the concentration of the added metal; the hardening is expressed by the quotient of the critical shear stress of the solid solution ($S_{0\,.\,\text{all.}}$) and that of the pure magnesium crystal (S_0): $\left(v_{\text{all.}} = \frac{S_{0\,.\,\text{all.}}}{S_0}\right)$. The increase of the shear stress is approximately linear with increasing content of foreign metal. The specific effect of the zinc greatly exceeds that of aluminium. The diagram also indicates the dependence upon concentration of the lattice parameters c and a, for both solid solutions. Corresponding to the smaller atomic radius of the added metals (Mg, 1·62 Å.; Al, 1·43 Å.; and Zn, 1·33 Å.) the lattice contracts in both cases. It is not yet clear whether the hardening effect of the zinc is connected with the greater reduction of c (*i.e.*, of the spacing of the glide planes) in the zinc–magnesium solid solutions.

Ternary aluminium–zinc–*magnesium* solid solutions (232) exhibited, at a concentration of $2{\cdot}5_4$ atomic-per cent. Al and 0·36 atomic-per cent. Zn, an $S_0 = 766$ g./mm.^{2}; and at a concentration of $5{\cdot}0_2$ atomic-per cent. Al and 0·38 atomic-per cent. Zn an $S_0 = 1153$ g./mm.^{2}.[1] These values were obtained by means of a good approximation from the behaviour of the two binary solid solutions on the assumption that the increases in the critical shear

[1] These are the technical alloys AZ.31 (with 2·8 per cent. Al and 0·9 per cent. Zn by weight), and AZM (with 5·6 per cent. Al and 1·0 per cent. Zn by weight).

stress due to the two alloying constituents were additive, and that consequently there was no reciprocal influence.

$$S_{0,\,\text{tern.}} - S_0 = (S_{0,\,\text{Al}} - S_0) + (S_{0,\,\text{Zn}} - S_0)$$

and therefore

$$v_{\text{all. tern.}} = v_{\text{all. Al}} + v_{\text{all. Zn}} - 1.$$

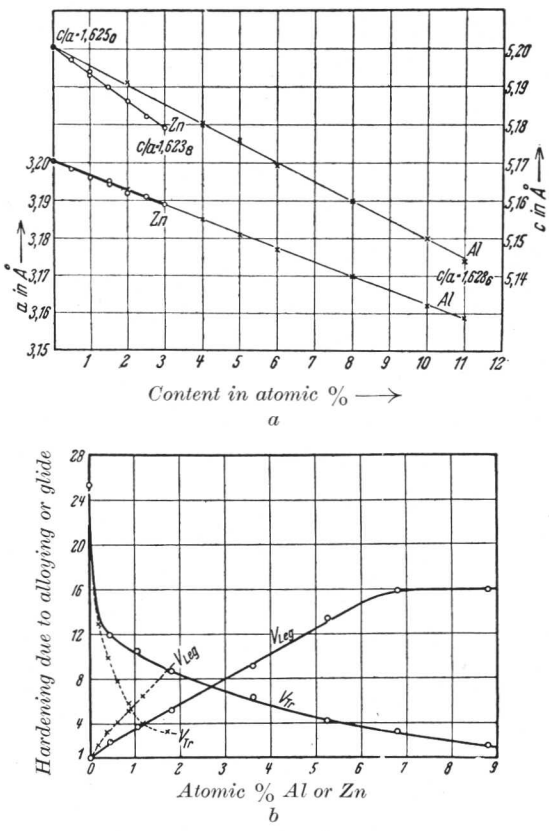

FIG. 102 (*a*) and (*b*).—Solid Solutions of Al–Mg and Zn–Mg.
(*a*) Lattice constants; (*b*) hardening as a function of concentration (231). $s_0 = 82{\cdot}9$ g./mm.². (N.B. In the text $v_{\text{Leg.}} = v_{\text{all.}}$)

This formula leads to $v_{\text{all. tern.}} = 8{\cdot}8$ for the first of the two alloys, and to $v_{\text{all. tern.}} = 14{\cdot}5$ for the second, whereas experimentally the values 9·2 and 13·9 were obtained. Thus if the saturation limit of

the ternary solid-solution region is known, it is possible to calculate, from the behaviour of the binary solid solutions, the concentration needed to give maximum shear resistance to the glide plane.

In the case of N additions, which do not substantially influence each other in their hardening effect, let it be assumed that the formula for calculating the hardening effect is

$$v_{\text{all.}} = v_{\text{all. A}} + v_{\text{all. B}} \ldots + v_{\text{all. N}} - (N - 1)$$

in which $v_{\text{all. A}} \ldots v_{\text{all. N}}$ represent the hardening of the appropriate

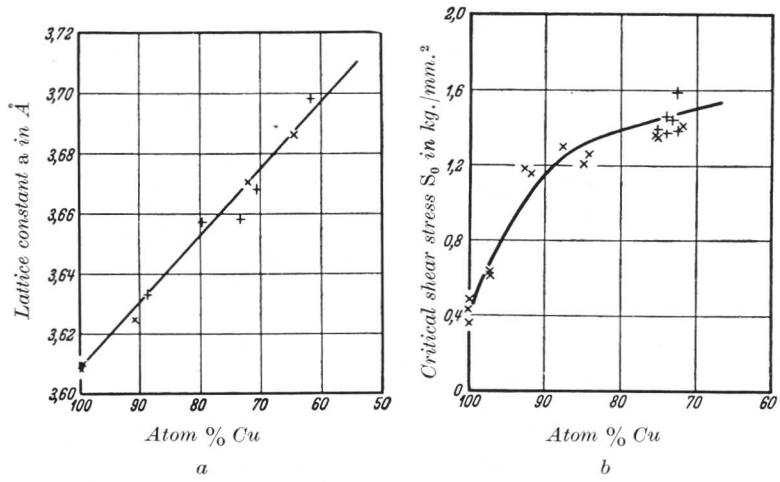

FIG. 103 (*a*) and (*b*).—α-Brass Crystals.

(*a*) Lattice constants [× (234), + (245), ● (246)]; (*b*) critical shear stress [× (234), + (233)] as a function of concentration.

binary series, which corresponds to an alloying metal content of A, . . .,N.

The hardening of cubic solid solutions is represented in Fig. 103 by the case of α-brass. Here the critical shear stress does not increase linearly with increasing concentration of the added metal; the greater the zinc content the smaller is the further increase in shear stress. The lattice constant indicated in the diagram shows an expansion due to the formation of the solid solution, and corresponding to the greater atomic radius of zinc (Cu, 1·27 Å.; Zn, 1·33 Å.). This expansion increases linearly with the atomic concentration. In the case of α-brass, therefore, hardening is bound up

with an increase in the spacing of the operative glide plane. At a zinc content of 18 atomic-per cent. the strength has increased approximately three-fold.

Fig. 104 contains the critical shear stress and the lattice constant for the complete silver–gold solid-solution series. The pure metal values are followed by a steep increase in the critical shear stress of

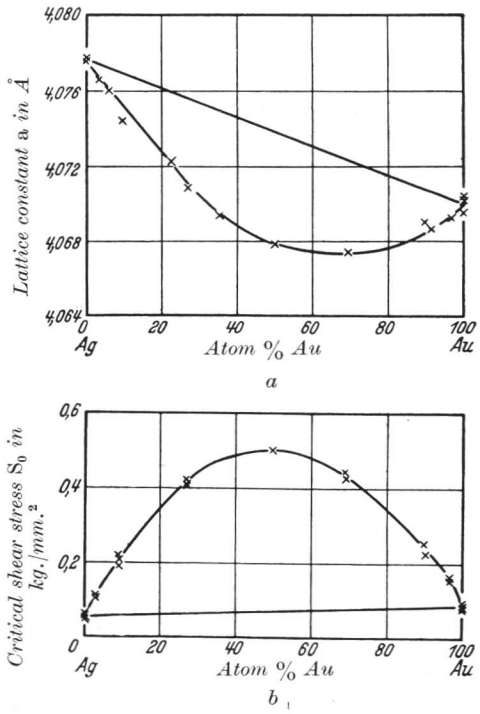

FIG. 104 (*a*) and (*b*).—Ag–Au Solid-solution Crystals.
(*a*) Lattice constants (247), (*b*) critical shear stress (235), as a function of concentration.

the octahedral glide system; the maximum is reached at approximately equal atomic concentration of both metals. The lattice constant exhibits a minimum at an intermediate concentration. A curve for critical shear stress similar to that shown in Fig. 104 has been obtained for the copper–nickel solid-solution series (236).

An instructive example of the significance of the *atomic arrangement* in the crystal for its plastic behaviour is found with gold–copper crystals, whose composition is given by the formula $AuCu_3$

(237). The disordered arrangement of the atoms at high temperature becomes ordered as the temperature falls; the cubic face-centred lattice, however, is retained (248). The appearance of superstructure lines corresponding to the ordered distribution is seen clearly in Fig. 105. The critical shear stress of these crystals falls

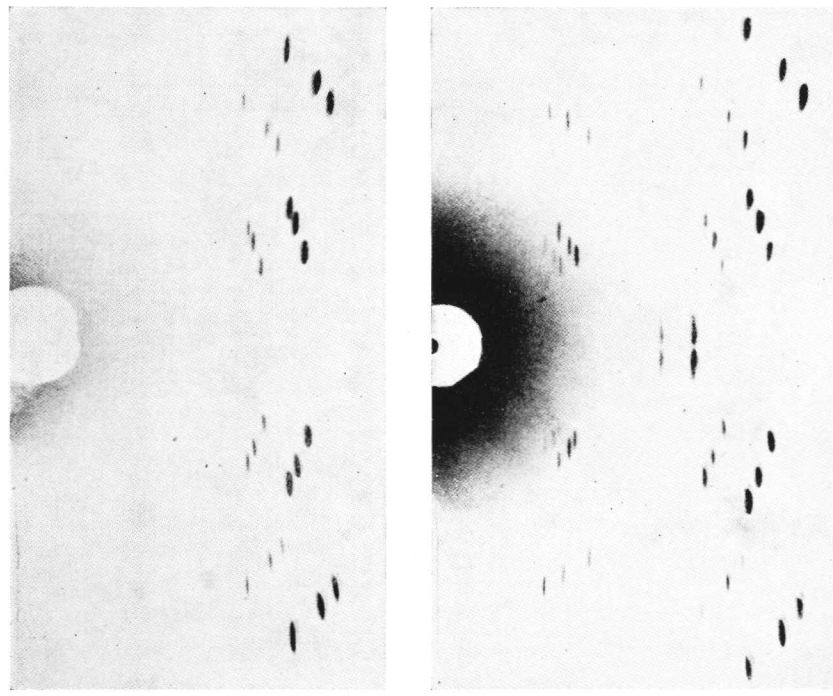

a *b*

FIG. 105 (*a*) and (*b*).—Rotation Photographs of a $AuCu_3$ Crystal (237).
(*a*) With random atomic distribution; (*b*) with ordered atomic distribution.

from 4·4 kg./mm.^{2} to 2·3 kg./mm.^{2} when passing from the disordered to the ordered arrangement.

The effect of *ageing* on the critical shear stress has been demonstrated by experiments carried out on crystals of an aluminium alloy with 5 per cent. copper (238), which, in the annealed state (slow cooling from 525° to 300° C., and kept at this temperature for an hour), gave a value of $S_0 = 1{\cdot}9$ kg./mm.^{2}, but after quenching from 525° C. followed by precipitation treatment for half an hour at

100° C., gave $S_0 = 9{\cdot}3$ kg./mm.^{2}. Fig. 106, referring to a quenched Al–Mg solid solution with 10 per cent. Al, shows the change in the

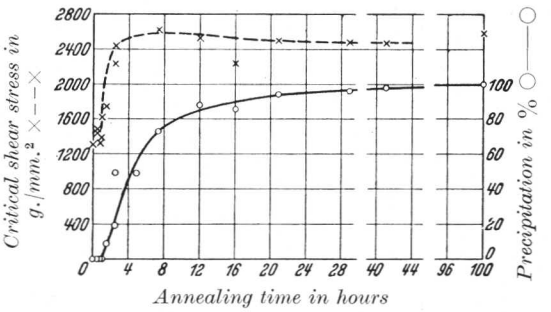

FIG. 106.—Shear Hardening and Precipitation (242). Supersaturated Al–Mg Solid Solution (10% Al) Annealed at 218° C. The "Precipitation" is the Amount of Al actually Precipitated (as Measured by Determination of the Lattice Constant) Expressed as a Percentage of the Amount Required to Establish Equilibrium.

critical shear stress of the basal plane as a function of the duration of heat treatment at 218° C. It is seen from the diagram, which also includes a curve giving the amount precipitated from the solid solution, that hardening and precipitation go hand in hand.

46. *Progress of Glide and Fracture in Alloy Crystals*

Fig. 107 contains extension curves of zinc crystals, of approximately similar orientation, alloyed with varying percentages of cadmium. They reveal once more the extremely strong dependence of the critical shear stress on the Cd content; they also show that the rate of hardening due to extension is less, the higher the original critical shear stress resulting from alloying. This reduction of the capacity for work hardening with increased initial hardening has been

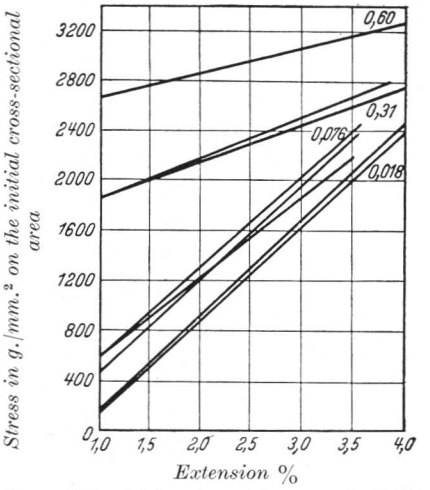

FIG. 107.—Extension Curves of Solid Solutions of Cd–Zn of Approximately Similar Orientation. Cd-content Given in Each Case in Atomic-% (230).

confirmed by all subsequent extension tests with alloy crystals [cf. curves in Fig. 102*b* with $v_{\mathrm{Tr}}\left(=\frac{S_{e,\,\mathrm{all.}}}{S_{0,\,\mathrm{all.}}}\right)$].

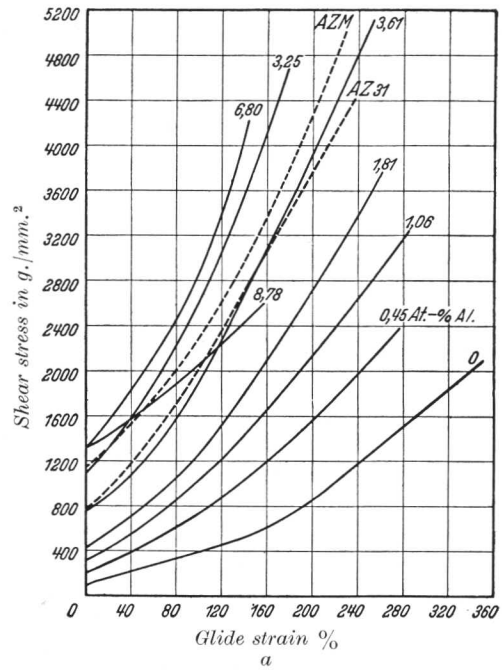

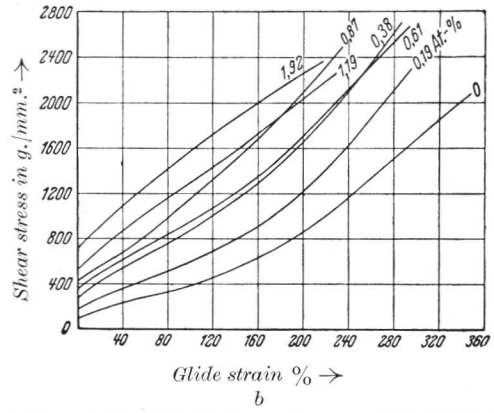

FIG. 108 (*a*) and (*b*).—Yield–Stress Curves of Mg Solid Solutions.
(*a*) Binary Al–Mg and ternary Al–Zn–Mg alloys (231, 232); (*b*) binary Zn–Mg alloys (231).